Nanoscale

Accepted Manuscript

This article can be cited before page numbers have been issued, to do this please use: W. Deng, L. Jin, Y. Chen, W. Chu, B. Zhang, H. Sun, D. Xiong, Z. Lv, M. Zhu and W. Yang, *Nanoscale*, 2017, DOI: 10.1039/C7NR07325A.

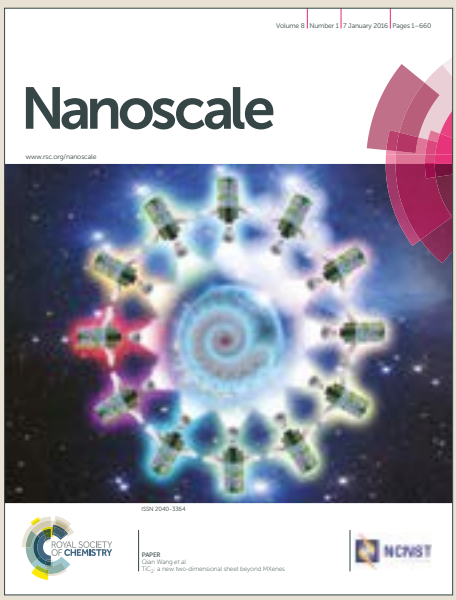

View Article Online
DOI: 10.1039/C7NR07325A

Nanoscale

ARTICLE

Enhanced Low-frequency Vibration ZnO nanorods-based Tuning Fork Piezoelectric Nanogenerator

Received 00th January 20 xx,
Accepted 00th January 20xx

DOI: 10.1039/x0xx00000x

www.rsc.org/

W. Deng,[a] L. Jin,[a] Y. Chen,[b] W. Chu,[b] B. Zhang,[a] H. Sun,[a] D. Xiong,[a] Z. Lv,[a] M. Zhu,[a,c] and W. Yang,[a,*]

In this paper, a piezoelectric nanogenerator (PENG) based on tuning fork-shaped cantilever was designed and fabricated, which aiming at harvesting low frequency vibration energy in the environment. In the PENG, a tuning fork-shaped elastic beam combined with ZnO nanorods (NRs), instead of conventional rectangular cantilever beams, was adopted to extract vibration energy. Benefiting from the high flexibility and the controllable shape of the substrate, this PENG was extremely sensitive to vibration and can harvest weak vibration energy at low frequency. Moreover, a series of simulation models were established to compare the performance of the PENG with different shapes. On this basis, the experimental results further verify that this designed energy harvester could operate at a low frequency which was about 13 Hz. The peak output voltage and current could respectively reach about 160 mV and 11 nA, and a maximum instantaneous peak power of 0.92 μW/cm^3 across a matched load of 9 MΩ was obtained. Evidently, this newly designed PENG could harvest vibration energy at lower frequency, which will contribute to broaden the application range of PENG in energy harvesting and self-powered system.

Introduction

With the miniaturization of modern electronic products, the development of microelectronic products has been seriously restricted due to the large size, limited life and the need for replacement of traditional batteries. How to realize the continuous power supply for this kind of low-power microelectronic products has become an urgent problem to be solved. The self-powered technology [1-8], which collects the other forms of energy from the environment to continuously supply low-power microelectronic devices, provides a good solution. Because of its ubiquity and abundance, vibration energy is the most widely studied energy source for energy-harvesting system [9]. According to the principle of operation, there are three kinds of energy harvesters, namely electrostatic, electromagnetic and piezoelectric, for converting vibration energy to electrical energy [10-12]. Due to the piezoelectric effect could convert any form of mechanical vibration into electrical energy, and has the advantages of simple structure, high energy density, no electromagnetic interference, and easy integration, PENG has attracted extensive attention of researchers in recent years [13-18].

Although the PENG could convert vibration energy to electric energy, the disadvantages of high resonance frequency and narrow working frequency band limited the application of PENG. To overcome these drawbacks, researchers have carried out lots of researches from two aspects of material synthesis and structural design [19-25]. Zheng *et al.* developed a cantilever using PZT sheets to convert energy, obtained the maximum electrical power of 32.5 μW at 211 Hz [26]. Tien *et al.* analyzed the prospective of PENG with piezocomposite, the maximum power could reach 0.22 mW at 310 Hz [27]. To further modify natural frequency of the piezoelectric energy harvester, Berdy *et al.* demonstrated a PENG using a meandering structure, resulted in the output power was 118 μW at 49.7 Hz [28]. In addition, Wen *et al.* designed and tested a spiral shaped cantilever using PVDF material, its resonance frequency could be lowered to about 20 Hz, but its maximal power output was only about 8.1 nW [29]. From the previous literature, it can be seen both the high Young's modulus of piezoelectric ceramics and the low piezoelectric coefficients of piezoelectric polymers limited the application of the PENG in low frequency field.

In this study, a tuning fork shaped PENG with ZnO nanorods has been adopted to provide an optimized power at lower work frequency. The key functional material of this design is the field-limited oriented ZnO NRs, which are grown on a flexible Kapton substrate through a low temperature hydrothermal method. The oriented ZnO NRs have better piezoelectric properties than membrane materials. More importantly, benefited from the discontinuity of ZnO NRs, the incidence of the shedding and fragmentation of the functional layer could be effectively reduced during vibration. Furthermore, the whole device was kept tuning fork shape, which could effectively lower the resonance frequency combined with flexible substrate. From the tested results, it can be seen that the designed PENG could work at a low

[a] Key Laboratory of Advanced Technologies of Materials (Ministry of Education), School of Materials Science and Engineering, Southwest Jiaotong University, Chengdu 610031, China. E-mail: wqyang@swjtu.edu.cn
[b] School of Mechanical Engineering, Southwest Jiaotong University, Chengdu 610031, China.
[c] State Key Laboratory of Traction Power, Southwest Jiaotong University, Chengdu 610031, China.

View Article Online
DOI: 10.1039/C7NR07325A

frequency about 13 Hz and the optimized maximum instantaneous peak power of 0.92 μW/cm^3 could be obtained, which provide a feasible method to improve the efficiency of energy harvester in low frequency field.

Structure Design and Simulation

The most common configuration of PENG is a cantilever with piezoelectric ceramic layers located on a vibrating host structure for electrical power generation from vibrations under resonance excitation [30]. Usually the substrate and the piezoelectric material were steel and piezoelectric ceramic respectively, both these two materials have higher Young's modulus resulting in higher natural frequency of the device. To solve this problem, we designed a new tuning fork shaped PENG as depicted in Fig. 1(a), which consists of a tuning fork shaped piezoelectric ZnO NRs based beam, copper electrodes and Kapton substrate. The vertical view and cross-sectional scanning electron microscopy (SEM) images of piezoelectric function material are respectively presented in Fig. 1 (b) and (c). The fabricated PENG shown in Fig. 1 (d) is available with the preparation process demonstrated in Fig. 1 (e).

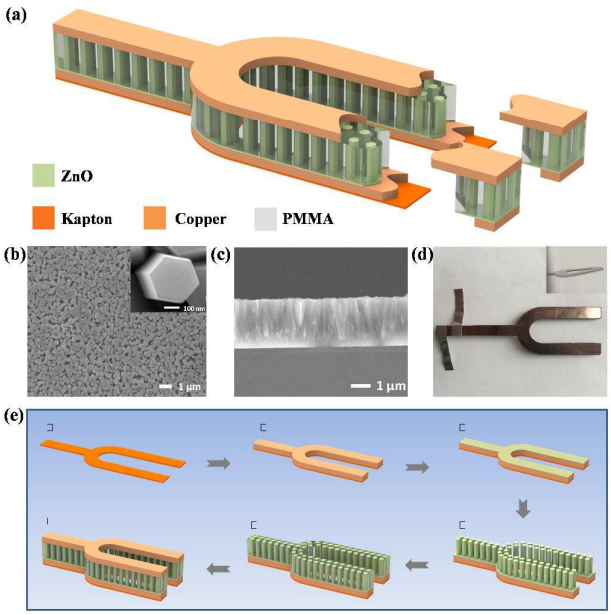

Fig. 1 Structural design of tuning fork shaped PENG. (a) The schematic diagram of tuning fork shaped PENG. (b) SEM image showing the ZnO NRs structure on the Kapton surface. The inset is a vertical view of the high-magnification image of individual ZnO NRs. (c) The cross-sectional SEM image of ZnO NRs on a Kapton substrate. (d) The photo of the fabricated PENG. The inset is a cross-sectional image the fabricated PENG. (e) Brief fabrication process of the fork featured PENG（I）Kapton substrate,（II）Bottom electrode,（III）ZnO seed layer,（IV）ZnO NRs,（V）Spin-coating PMMA,（VI）Top Electrode.

Compared with traditional PENG, the proposed structure has many advantages. Firstly, the Kapton substrate is a flexible substrate [31], which has a smaller Young's modulus, theoretically it will have a lower resonant frequency. Secondly, the piezoelectric material is ZnO NRs [32, 33], which has the advantages of simple manufacturing process, low cost, no sintering and no polarization [34-36]. Lastly, compared with the traditional piezoelectric functional film, a small gap between the NRs, leading to the discontinuity of the entire piezoelectric functional layer, can effectively reduce the occurrence of fragmentation or abscission of materials and then the device could show better robustness.

In order to verify the validity of our design, we carry out the simulation through a finite element method (FEM) [37]. Typically, cantilever type PENG is rectangular in shape with or without a proof mass attached at the free end [38]. At present, most of the mathematical models of this kind energy harvester are the equivalent models proposed by Williams and Yates [39]. According to the equivalent model, when the external excitation frequency is equal to the natural frequency of the device, that is the resonance occurs, the device has the maximum power output. And the dimensions of the cantilever decides the natural frequency of the harvester, therefore, we respectively compared different shapes of cantilever, rectangle, triangle and tuning fork, to verify that if the designed structure can effectively reduce the natural frequency. To make the results comparable, all parameters in simulation model are kept consistent except shape, including the length of 5 cm, the cantilever beam thicknesses of 0.1 mm, piezoelectric function layer of 0.01 mm, the total areas of 5 cm^2, and the lengths of the fixed part was 1 cm. The simulation results of PENG with different structures are shown in Fig. 2.

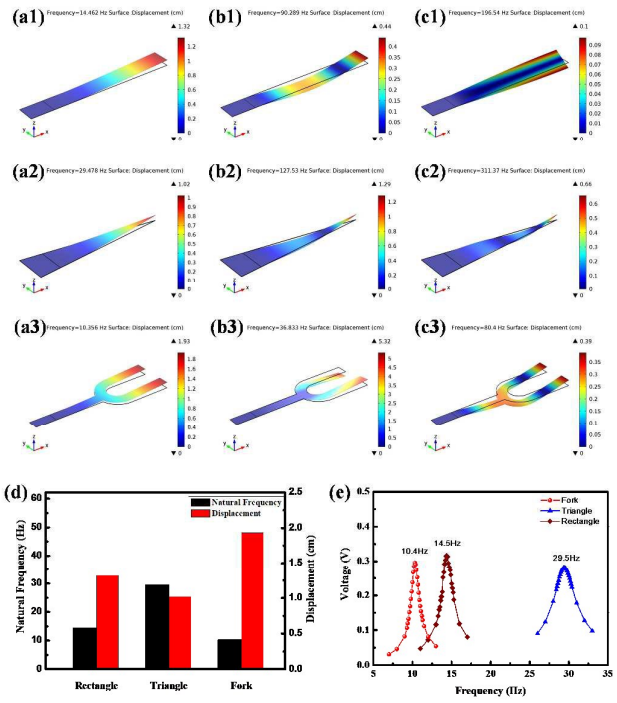

View Article Online
DOI: 10.1039/C7NR07325A

Fig. 2 The simulation results of PENG with different structures. The first-order (a1), second-order (b1), third-order (c1) modal maps of rectangular energy harvester; The first-order (a2), second-order (b2), third-order (c2) modal maps of triangular energy harvester; The first-order (a3), second-order (b3), third-order (c3) modal maps of fork structured energy harvester; The comparison of natural frequency, displacement (d) and voltage output (e) of energy harvester with different shapes.

The deformation of different structures under different vibration modes can be clearly seen from Fig. 2. Generally, devices are most likely to work at the first order resonant frequency [40], therefore, we further discuss the performance of the device at the first order resonant frequency, and the quantitative results are exhibited in Fig. 2 (d-e). From the results, it is easy find that tuning fork shaped PENG has the maximal displacement and the lowest natural frequency compared with the other two structures. Moreover, there is little difference in voltage output among the three structures at the resonant frequency points, but the resonant frequency of the tuning fork is obviously lower than the other two structures. Therefore, the better output can be obtained by adopting the tuning fork shaped PENG, which verify the correctness of the design.

Results and Discussion

In the experiment, the morphology of the ZnO NRs grown on the surface of the Kapton film via a hydrothermal method is shown in Fig. 1(b). From the SEM image, it can be observed that the NRs grew radially on the Kapton film with almost identical morphology and dense coverage over the surface of the substrate. The inset is a vertical view of a high-magnification image, obviously presenting a regular hexagonal cross-section of the ZnO NR with a diameter about 300 nm. The lengths around 2.4 μm could be obtained from the cross-section view of ZnO NRs layer presented in Fig. 1(c). And the XRD patterns of ZnO NRs are shown in Fig. S1. From the results, it can be seen the strongest peaks appear at ~ 34.5°, which is indexed to (002) plane of hexagonal ZnO crystal. This is in good agreement with the hexagonal shape of ZnO NRs (Fig. 1b), and indicates that ZnO NRs have a strong *c*-axis orientation. These oriented ZnO NRs provide two opposite polar surfaces, resulting in a normal dipole moment and spontaneous polarization along the *c*-axis [32]. Thus, the output of electrical performance could be improved through this design. Furthermore, the separation of the ZnO NRs combined with PMMA layer [41] improves the stress distribution at the interface under vibration, signifying a long working lifetime and stability.

In order to further investigate the electrical output performance of the as-fabricated tuning fork shaped PENG, an electromechanical vibrator was used to simulate external vibration excitation, and the schematic diagram of the test system is shown in Fig. 3(a). The quantitative characterization of the output performance of the PENG could be acquired through the measure meters and data acquisition system. For a PENG, the maximum output voltage is primarily determined by the piezoelectric voltage constant for a given applied load or impact energy [42]. Hence, during the testing of electronic properties, the amplitude of the vibrator remains constant and the frequency of the vibrator increases linearly. The corresponding typical electrical output characteristics of the energy harvester are presented in Fig. 3. From the figure, it can be seen that the open-circuit voltages (Fig. 3 b) and short-circuit current (Fig. 3 c) present sinusoidal curve, which are in good agreement with harmonic vibration of vibrator. With the increase of frequency, the open-circuit voltages (Fig. 3 d) and short-circuit current (Fig. 3 e) both firstly increase and then decline. In addition, the peak values of the open-circuit voltage and the short-circuit current respectively reach up to 160mV and 11nA at 13 Hz, indicating that 13 Hz is the resonance frequency of the fabricated PENG.

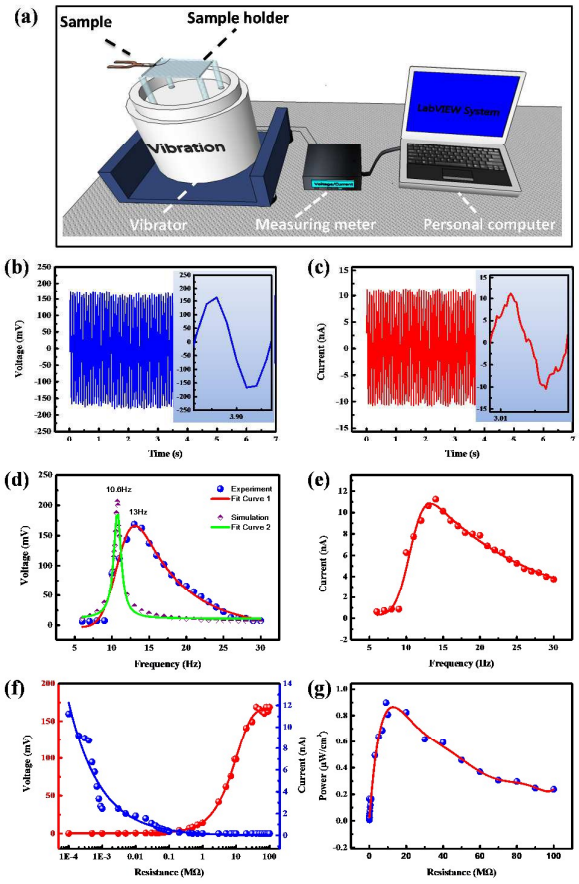

Fig. 3 Electrical output characterization of the fabricated PENG. (a) The schematic diagram of the measurement platform of PENG. The open circuit voltage (b) and short circuit current (c) change with time. The voltage (d) and current (e) response with frequency. The voltage and current response curve (f) and the instantaneous peak power curve (g) as a function of resistance.

The experimentally measured natural frequency and output voltage are compared to the FEM simulated results illustrated

View Article Online
DOI: 10.1039/C7NR07325A

in Fig. 3 (d). As can be seen, the theoretical maximum open-circuit voltage and resonance frequency are 207 mV and 10.6 Hz, respectively. Compared with the peak value of the measured results of 160 mV and 13 Hz, obviously, both two values exhibited some deviations between the numerical and experimental results. Analysis of the reasons, due to the mechanical processing of the substrate, it is easy to bring machining deformation caused by the existence of the residual stress, which will change the natural frequency of the device. On the other hand, not all ZnO NRs are perfectly aligned and grow along the *c* axis in the experiment, but the setting of simulation is ideal. Hence, there are some differences between the experimental and the simulation results.

The further evolutions of the output electrical performance with the load resistance are plotted in Fig. 3 (f-g). As displayed in Fig. 3 (f), the instantaneous current density amplitude drops with increasing load resistance owing to the resistive loss, while the voltage follows a build-up trend. Consequently, the global maximum of the instantaneous peak power occurs when the load resistor is about 9 MΩ, corresponding to a peak power of about 0.92 μW/cm^3 (Fig. 3 g), revealing that the optimal matching impedance of the fabricated PENG is 9 MΩ.

Conclusions

In summary, this work presented a tuning fork shaped PENG to enhance energy conversion efficiency at lower frequency. The designed PENG was proved to have better performance than other two structures through a series of FEM models. Meanwhile, the demo was fabricated to further verify the performance. As the experimental results showed, the peak values of the open-circuit voltage and the short-circuit current respectively reach up to 160 mV and 11 nA at 13 Hz, and a maximum instantaneous peak power of 0.92 μW/cm^3 across a matched load of 9 MΩ was obtained. With major advantages such as simple manufacturing process, low cost, no sintering and no polarization, our newly designed PENG provides a new approach for harvesting low-frequency vibration energy, and which will have a wide application space in energy self-powered system.

Experimental Details

In order to obtain the presented tuning fork shaped PENG, a series of processing technology were used. The detailed fabrication process is displayed in Fig. 1(e). Firstly, the flexible Kapton substrate was cut to the tuning fork shape with the mask. Then a copper layer about 300 nm was deposited on the fabricated substrate through magnetron sputtering to serve as the bottom electrode. Next, a ZnO film about 100 nm was deposited on the bottom electrode through evaporation technique to serve as the seed layer. After that, the ZnO-seed-coated Kapton film was immersed into a nutrient solution to growth ZnO via a low temperature hydrothermal method [43]. The nutrient solution we used in the chemical growth process was an aqueous solution of $Zn(NO_3)_2$▪$6H_2O$ and HMTA (hexamethylenetetramine), and the concentration was 0.1 M [44], which was carried out in a convection oven at 85 °C for 6 hours. At the end of the reaction, the Kapton film was taken out of the solution, rinsed with DI (deionized) water, and then dried. The next step, a thin layer of PMMA (polymethyl methacrylate) was spin-coated on the surfaces of the substrate at the speed of 3000 rpm [41]. Finally, another copper layer was deposited on the Kapton film to serve as the top electrode behind the PMMA was dried. After the wires were drawn from the top electrode and the bottom electrode respectively, the device was ready to work. The vibration of the device was controlled by a programmable shaker (Dongling ESS-025). The open-circuit voltage was measured using a Keithley 6514 system electrometer, and the short-circuit current was measured using an SR570 low noise current amplifier (Stanford Research System).

Acknowledgements

This work is supported by the Fundamental Research Funds for the Central Universities (No. 2682017CX071), Sichuan Province Science and Technology Plan Project (No. 2015JQ0013), Sichuan Province Youth Science and Technology Innovation Team (No. 2016TD0026) and the Independent Research Project of State Key Laboratory of Traction Power (No. 2016TPL_Z03 and 2017TPL_Z04).

Notes and references

1 Z. L. Wang, *Adv. Funct. Mater.*, 2010, 3553-3567.
2 L. Zhang, B. Zhang, J. Chen, L. Jin, W. Deng, J. Tang, H. Zhang, H. Pan, M. Zhu, W. Yang and Z. L. Wang, *Adv. Mater.*, 2016, **28**, 1650-1656.
3 B. Zhang, J. Chen, L. Jin, W. Deng, L. Zhang, H. Zhang, M. Zhu, W. Yang and Z. L. Wang, *ACS Nano*, 2016, **10**, 6241-6247.
4 L. Jin, J. Chen, B. Zhang, W. Deng, L. Zhang, H. Zhang, X. Huang, M. Zhu, W. Yang and Z. L. Wang, *ACS Nano*, 2016, **10**, 7874-7881.
5 B. Zhang, L. Zhang, W. Deng, L. Jin, F. Chun, H. Pan, B. Gu, H. Zhang, Z. Lv and W. Yang, *ACS Nano*, 2017, **11**, 7440-7446.
6 L. Jin, W. Deng, Y. Su, Z. Xu, H. Meng, B. Wang, H. Zhang, B. Zhang, L. Zhang and X. Xiao, *Nano Energy*, 2017, **38**, 185-192.
7 K. Liu, Y. Zhou, F. Yuan, X. Mo, P. Yang, Q. Chen, J. Li, T. Ding and J. Zhou, *Angew. Chem.*, 2016, **55**, 15864-15868.
8 T. Ding, K. Liu, J. Li, G. Xue, Q. Chen, L. Huang, B. Hu and J. Zhou, *Adv. Funct. Mater.*, 2017, **27**, 1700551.
9 S. P. Beeby, M. J. Tudor and N. M. White, *Meas. Sci. Technol.*, 2006, **17**, 175-195.
10 S. Saadon and O. Sidek, *Energy Convers. Manage.*, 2011, **52**, 500-504.
11 A. Harb, *Renew. Energy*, 2011, **36**, 2641-2654.
12 C. R. Bowen, H. A. Kim, P. M. Weaver and S. Dunn, *Energy Environ. Sci.*, 2014, **7**, 25-44.
13 Z. Chen, B. Guo, Y. Yang and C. Cheng, *Physica B*, 2014, **438**, 1-8.
14 X. Zhang, P. Pondrom, L. Wu and G. Sessler, *Appl. Phys. Lett.*, 2016, **108**, 193903.
15 A. Toprak and O. Tigli, *Appl. Phys. Rev.*, 2014, **1**, 031104.
16 R. Ahmed, F. Mir and S. Banerjee, *Smart Mater. Struct.*, 2017, **26**, 085031.
17 B. Kumar and S.-W. Kim, *Nano Energy*, 2012, **1**, 342-355.
18 J. X. Zhao, J. Yang, Z. W. Lin, N. Zhao, J. Liu, Y. M. Wen and P. Li, *Sensor Actuat A-Phys.*, 2015, **236**, 173-179.

View Article Online
DOI: 10.1039/C7NR07325A

19 H. Li, L. Su, S. Kuang, Y. Fan, Y. Wu, Z. L. Wang and G. Zhu, *Nano Res.*, 2017, **10**, 785-793.
20 J.-H. Lee, J. Kim, T. Y. Kim, M. S. Al Hossain, S.-W. Kim and J. H. Kim, *J. Mater. Chem. A*, 2016, **4**, 7983-7999.
21 H. Li, C. Tian and Z. D. Deng, *Appl. Phys. Rev.*, 2014, **1**, 041301.
22 M.-G. Kang, W.-S. Jung, C.-Y. Kang and S.-J. Yoon, *Actuators*, 2016, **5**, 5.
23 J. Twiefel and H. Westermann, *J. Intel. Mater. Syst. Struct.*, 2013, **24**, 1291-1302.
24 H. H. Huang and K. S. Chen, *Sensor Actuat A-Phys.*, 2016, **238**, 317-328.
25 A. Jemai, F. Najar, M. Chafra and Z. Ounaies, *Compos. Struct.*, 2016, **135**, 176-190.
26 Q. Zheng and Y. Xu, *Smart Mater. Struct.*, 2008, **17**, 055009.
27 C. M. T. Tien and N. S. Goo, *J. Intel. Mater. Syst. Struct.*, 2010, **21**, 1427-1436.
28 D. F. Berdy, P. Srisungsitthisunti, B. Jung, X. Xu, J. F. Rhoads and D. Peroulis, *IEEE T. Ultrason. Ferr.*, 2012, **59**, 846-858.
29 W. Liu, M. D. Han, B. Meng, X. M. Sun, X. L. Huang and H. X. Zhang, *Sci. China Technol. Sci.*, 2014, **57**, 1068-1072.
30 C. Wei and X. Jing, *Renew. Sust. Energy Rev.*, 2017, **74**, 1-18.
31 P. Bai, G. Zhu, Y. S. Zhou, S. Wang, J. Ma, G. Zhang and Z. L. Wang, *Nano Res.*, 2014, **7**, 990-997.
32 Z. L. Wang, Appl. Phys. A: Mater. Sci. Process., 2007, **88**, 7-15.
33 J. Zhao, X. Yan, Y. Yang, Y. Huang and Y. Zhang, *Mater. Lett.*, 2010, **64**, 569-572.
34 Y. Yang, J. Qi, Q. Liao, H. Li, Y. Wang, L. Tang and Y. Zhang, *Nanotechnology*, 2009, **20**, 125201.
35 N. Ye, J. Qi, Z. Qi, X. Zhang, Y. Yang, J. Liu and Y. Zhang, *J. Power Sources*, 2010, **195**, 5806-5809.
36 Y. Yang, J. Qi, W. Guo, Y. Gu, Y. Huang and Y. Zhang, *Phys. Chem. Chem. Phys.*, 2010, **12**, 12415-12419.
37 R. Tao, G. Ardila, L. Montès and M. Mouis, *Nano Energy*, 2015, **14**, 62-76.
38 S. S. Balpande, R. S. Pande and R. M. Patrikar, *Sensor Actuat A-Phys.*, 2016, **251**, 134-141.
39 C. B. Williams and R. B. Yates, *Sensor Actuat A-Phys.*, 1996, **52**, 8-11.
40 H. S. Kim, J.-H. Kim and J. Kim, *Int. J. Precis. Eng. Man.*, 2011, **12**, 1129-1141.
41 G. Zhu, A. C. Wang, Y. Liu, Y. Zhou and Z. L. Wang, *Nano Lett.*, 2012, **12**, 3086-3090.
42 X. Chen, S. Xu, N. Yao and Y. Shi, *Nano Lett.*, 2010, **10**, 2133.
43 W. Deng, L. Jin, B. Zhang, Y. Chen, L. Mao, H. Zhang and W. Yang, *Nanoscale*, 2016, **8**, 16302-16306.
44 Y. Hu, Y. Zhang, C. Xu, L. Lin, R. L. Snyder and Z. L. Wang, *Nano Lett.*, 2011, **11**, 2572-2577.

View Article Online
DOI: 10.1039/C7NR07325A

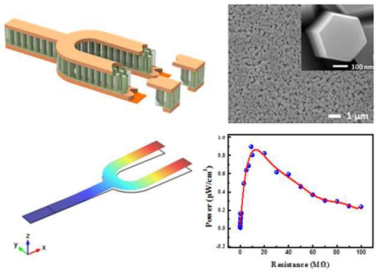

Enhanced piezoelectric nanogenerator from low-frequency vibration utilizing ZnO nanorods-based tuning fork